Forest Ecology and Management 490 (2021) 119128

Contents lists available at ScienceDirect

Forest Ecology and Management

journal homepage: www.elsevier.com/locate/foreco

Climate, drought and hydrology drive narrow-leaved ash growth dynamics in southern European riparian forests

Patricia M. Rodríguez-González [a], Michele Colangelo [b,c], Ángela Sánchez-Miranda [d], Raúl Sánchez-Salguero [b,d], Filipe Campelo [e], Angelo Rita [c,f], Inês Gomes Marques [a], António Albuquerque [g], Francesco Ripullone [c], J. Julio Camarero [b,*]

[a] Forest Research Centre, School of Agriculture, University of Lisbon, Lisbon 1349-017, Portugal
[b] Instituto Pirenaico de Ecología (IPE-CSIC), Avda. Montañana 1005, E-50192 Zaragoza, Spain
[c] Scuola di Scienze Agrarie, Forestali, Alimentari e Ambientali, Università della Basilicata, Viale dell'Ateneo Lucano 10, 85100 Potenza, Italy
[d] Departamento de Sistemas Físicos, Químicos y Naturales, Universidad Pablo de Olavide, 41013 Sevilla, Spain
[e] Centre for Functional Ecology, Department of Life Sciences, University of Coimbra, Calçada Martim de Freitas, 3000-456 Coimbra, Portugal
[f] Dipartimento di Agraria, Università di Napoli Federico II, via Università 100, 80055 Portici, NA, Italy
[g] ECOFIELD, Monitorizações, Estudos e Projectos, Lda., Est de Polima 673, Moradia 1.°, 2785-543 São Domingos de Rana, Cascais, Portugal

ARTICLE INFO

Keywords:
Dendroecology
Drought
Fraxinus angustifolia
Radial growth
River hydrology
Tree rings

ABSTRACT

Mediterranean riparian forests are among the most threatened ecosystems in Europe. These ecosystems are exposed to land-use changes threatening their reduced habitat and by global warming, which is already triggering aridification processes. To assess the impact of these major threats, we studied the radial-growth responses to climate and drought in the narrow-leaved ash (*Fraxinus angustifolia*). This riparian tree species presents a relatively large ecological spectrum in its habitat preference in the Mediterranean Basin. We studied five sites arranged across a wide geographical range from Iberia to Italy, subjected to contrasting climatic conditions and located in hydrographic basins with different sizes and water regimes. We found diverse growth responses to climate and drought across the Mediterranean distribution range of the narrow-leaved ash at the individual and site levels. The growth of this species increased in response to wet and cool conditions in the prior winter and spring. The response to summer conditions was only observed in the coldest and wettest site (Ticino). Growth responded negatively to 2–14 month droughts that occurred from previous winter up to summer, particularly in the warmest-driest sites. Growth responses to drought peaked in the warmest-driest sites in terms of climate water balance (Odelouca, Doñana), but not in the driest sites in terms of annual precipitation (Tudela, Zaragoza). Hydrological conditions also affected the narrow-leaved ash with high discharges in the prior winter and early spring enhancing wood production. Considering projected aridification and increased hydrological alteration, implying limited water supply in the Mediterranean region, climate warming will negatively impact productivity of narrow-leaved ash riparian forests. Further research should combine analyses of growth responses to climate and hydrology from tree to basin scales to disentangle their relative roles as drivers of productivity under different scenarios of climate and hydrological changes, in order to aid adaptive management of these key ecosystems.

1. Introduction

In climate-change hotspots such as the Mediterranean Basin drought is becoming a major driver of productivity and tree growth changes in riparian and floodplain forests (Gomes Marques et al., 2018, Stella and Bendix, 2019). Climate warming and land-use changes can interact and further threaten riparian forest ecosystems by exacerbating aridification, altering hydrological regimes and contributing to the expansion of pathogens (Rodríguez-González et al. 2010, 2014, Dufour et al., 2018, Adamcikova et al., 2018). In this region, but also in wetter central and

* Corresponding author.
E-mail addresses: patri@isa.ulisboa.pt (P.M. Rodríguez-González), rsanchez@upo.es (R. Sánchez-Salguero), fcampelo@uc.pt (F. Campelo), angelo.rita@unibas.it (A. Rita), icgmarques@isa.ulisboa.pt (I. Gomes Marques), aalbuquerque@ecofield.pt (A. Albuquerque), francesco.ripullone@unibas.it (F. Ripullone), jjcamarero@ipe.csic.es (J.J. Camarero).

https://doi.org/10.1016/j.foreco.2021.119128
Received 30 November 2020; Received in revised form 4 February 2021; Accepted 1 March 2021
Available online 19 March 2021

northern Europe, growth decline, canopy dieback and elevated mortality have been described in major riparian tree species such as black alder (*Alnus glutinosa* (L.) Gaertn.) (Valor et al. 2020) and common ash (*Fraxinus excelsior* L.) (Enderle et al., 2019, Hultberg et al., 2020, Klesse et al., 2020).

Tree growth and productivity of riparian forests depend on hydrologic and climatic regimes of the catchment which regulate relevant functional aspects, such as the canopy evaporative demand, the water table depth and soil water availability (Stella et al., 2013). In particular, droughts can trigger a drop in water table and limit the access of trees to soil water, leading to growth decline (Andersen, 2016), increasing tree mortality (Scott et al., 1999, Tulik et al., 2020). Intense and long droughts negatively impact riparian and floodplain forests, specifically tree species with a low plasticity in root system depth (Garssen et al., 2014). However, this was concluded based on meta-analyses carried out with seedlings, illustrating our poor knowledge of the long-term growth responses to climate, drought and hydrological changes in adult trees of major riparian tree species (but see Stromberg and Patten, 1996, Scott et al., 2000, Cailleret et al., 2019). A better understanding of radial-growth responses to climate and drought in Mediterranean riparian forests is required to project their dynamics under climate change, and also to better manage these threatened forest ecosystems and related water resources (García-Ruiz et al., 2011, Gomes Marques et al., 2018).

In the Mediterranean region, the narrow-leaved ash (*Fraxinus angustifolia* Vahl) replaces the common ash and mainly appears in cool-wet sites along rivers, their floodplains and wetlands, being part of mixed broadleaved forests (Caudullo et al., 2016). It grows on sites with moist soils, in temporary flooded lowlands, but also on well-drained slopes at cold, high-elevation sites forming mixed stands with other broadleaved species such as cottonwoods, oaks and elms (Caudullo et al., 2016). In addition to hydroclimatic factors (Rodríguez-González et al., 2008), the narrow-leaved ash development also responds to soil structure and composition (Gomes Marques et al., 2018), making this species potentially dominant in less local water-dependent habitats within floodplains.

The narrow-leaved ash shows a relatively large ecological spectrum, both in bioclimatic setting and in hydrological requirements, spanning from strictly riparian to transitional upland forests (Gomes Marques et al., 2018). Thus, studying growth dynamics of this species across southern Europe allows characterizing the responses of a major riparian tree species across a large environmental range and to forecast dynamics and post-drought resilience of threatened Mediterranean riparian ecosystems (Stella et al., 2013). These forecasts are important to get insight into climate-growth response and predict future Mediterranean ash forests distribution, which over the last centuries experienced a great reduction due to conversion of floodplain forests into agricultural fields (EEA, 2015). Several studies conducted in southern Iberia recently acknowledged the importance of ongoing rising temperature due to climate change and increased pressure on water resources in triggering productivity changes (Rodríguez González et al., 2017, Gomes Marques et al., 2018). These changes might potentially contribute to composition shifts in the remaining floodplain ash stands (Rodríguez González et al., 2017; Gomes Marques et al., 2018).

To the best of our knowledge, there are yet no studies investigating the variability in growth response of narrow-leaved ash stands to different climatic conditions across different hydrologic settings. Here we quantified past radial-growth dynamics by using dendrochronology (Fritts, 1976) and assessed how climate and hydrology impacted growth. Specifically, we aimed: (i) to reconstruct radial-growth patterns of narrow-leaved ash populations in five sites located across the central and western Mediterranean Basin, (ii) to quantify climate- and drought-growth relationships, and (iii) to evaluate the relative importance of seasonal climate variables, tree age and diameter as drivers of radial growth. As ash species are characterized by a shallow root system and tend to use surface soil water (Singer et al 2013), we hypothesized that the growth responses to warm-dry climate conditions and drought would be more marked in drier than in wetter sites, and these responses would be modulated by warmer growing-season temperatures enhancing evapotranspiration rates.

2. Materials and methods

2.1. Study sites

The five study sites were selected such that they covered contrasting environmental conditions where the narrow-leaved ash occurs (Table 1). Three of them were located in Spain, one in southern Portugal and the other in northern Italy (Fig. 1). We sampled two sites situated near the cities of Zaragoza and Tudela in the Ebro basin, which is located in the north-eastern Iberian Peninsula, occupying a total surface of 85,362 km^2 and representing the largest hydrographic basin in Spain and the third one in surface of the Mediterranean. These two sites are situated in the Middle Ebro basin, where the river has a low longitudinal slope and forms meandering channels (Ollero, 2007). Two relatively well-preserved floodplain forests were considered: Soto de la Remonta (near Tudela, Navarra region) and Soto de Partinchas (near Zaragoza, Aragón region), which experienced past local disturbances such as the building of local dikes in the 1950s and 1960s, particularly near the Zaragoza site (Ollero, 1990). The Tudela site shows free-flowing river dynamics and a forest structurally more diverse than the Zaragoza site (Ayerra, 1988). Climate in this area is semi-arid Mediterranean continental. The coldest and warmest months are January (5.4–5.6 °C) and July (22.7–23.6 °C), respectively. A pronounced summer dry period lasts from June to September. The Ebro river flows into the Iberian Depression, with marl and gypsum Miocene deposits in some areas. Soils are basic and of the loamy-sandy type. Reservoirs mainly built since the 1950s have smoothed the Ebro river flow regime, reducing the higher winter flows and alleviating the low water levels in summer (Frutos et al., 2004). These forests are dominated by tamarisks (*Tamarix* spp.), white willow (*Salix alba* L.) and silver poplar (*Populus alba* L.) situated near the river bank, black poplar (*Populus nigra* L.) located in the transition zone, and narrow-leaved ash with scattered elm trees (*Ulmus minor* Mill.) in the understory, often affected by Dutch elm disease, situated inland.

The Doñana study site (Andalusia, southern Spain) is situated along the floodplain forest of "La Rocina", a tributary stream of 19 km length feeding from its western part the Doñana marshes which are located at the downstream section of the Guadalquivir river basin. La Rocina collects runoff and groundwater along a sandy catchment of around 400 km^2. The average annual water discharge from La Rocina to the Doñana marshes has been reported about 40 hm^3 (Manzano et al., 2005). The Doñana study site has a Mediterranean sub-humid climate (rainy autumns and winters, hot and dry summers and mild winters) with mean annual precipitation of 549 mm and mean annual temperature of 18.1 °C, ranging from 4.6 °C in January to 32.6 °C in July. In this site, the flood cycle starts in September and usually reaches the maximum in late winter, with this peak being subject to high rainfall variability. Clay and silt substrates predominate in the Doñana marshes which are soaked with the first rains and a shallow water layer spreads over the flooded area. The tributary river network streams into the marshes maintaining water levels as runoff flows through their catchments. The marshes are included in the Doñana National Park, yet, La Rocina floodplain forests and a surrounding 500 m buffer have a minor protection status, limited to the downstream 12 km. The floodplain forest is mainly dominated by narrow-leaved ash colonizing the transitional areas between highly flooded sites, which are dominated by *Salix atrocinerea* Brot. (Rodríguez González et al., 2017).

The Odelouca study site is located in Odelouca river, a tributary of Arade hydrographic basin, located in Algarve Region, southern Portugal. The Odelouca basin has 511 km^2 of drainage area and 92 km of slow-running streams, with a mostly natural (free-flowing) Mediterranean flooding regime at the time of the sampling. Mean annual

Table 1
Sites' geographical and climatic characteristics. Climatic data was obtained from European 0.25°-gridded E-OBS-v13.1 dataset (Cornes et al., 2018). The last column shows the climatic moisture index (CMI) dry (wet) sites showing negative (positive) CMI values.

Site	Country	Latitude (N)	Longitude	Elevation (m a.s.l.)	Mean annual temperature (°C)	Total annual precipitation (mm)	CMI
Odelouca	Portugal	37°14′	8°30′W	120	16.9	750	−0.43
Doñana	Spain	37°06′	6°39′W	69	18.1	549	−0.60
Zaragoza	Spain	41°42′	0°56′W	205	14.7	357	−0.38
Tudela	Spain	42°07′	1°35′W	257	13.9	485	−0.33
Ticino	Italy	45°26′	8°50′E	202	12.6	1030	0.17

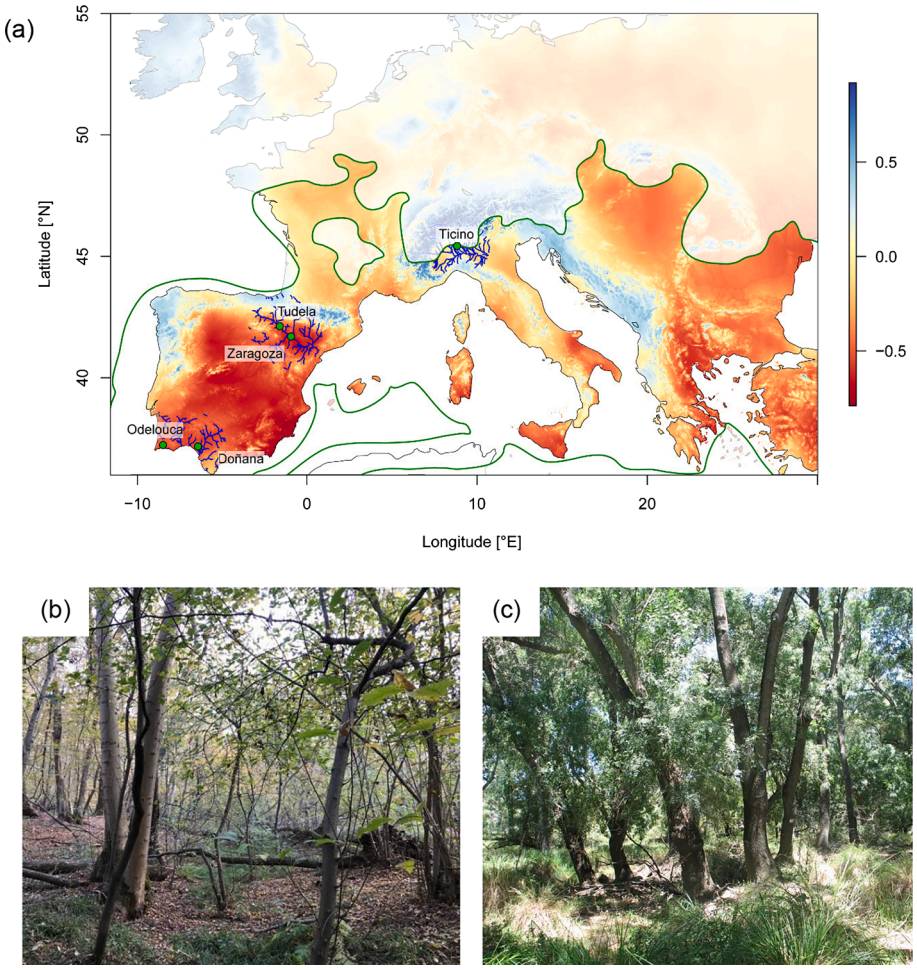

Fig. 1. Map with the five ash sites sampled in southern Europe (a) and views of the Ticino (b) and Doñana (a) study sites. In the upper map, the green line delimits the distribution area of the narrow-leaved ash (*Fraxinus angustifolia*) in the Mediterranean Basin, whereas the color scale shows the climate moisture index (CMI) with wet and dry sites climates showing positive or negative CMI values, respectively. The blue thick lines in the map represent the hydrographic networks of the sampled ash stands (a). (For interpretation of the references to color in this figure legend, the reader is referred to the web version of this article.)

precipitation is around 750 mm, mostly concentrated in a wet period from October to April, contrasting with a very dry period from June to September. The monthly temperatures range between 11.6 °C (January) and 23.1 °C (August). The main substrates of the drainage basin are sedimentary and metamorphic formations, in particular clay shales, greywacke and sandstones. The riparian forests at the Odelouca basin, are mainly dominated by narrow-leaved ash, willow (*Salix salviifolia* Brot.), tamarisk (*Tamarix africana* Poir), oleander (*Nerium oleander* L.) and alder (*A. glutinosa*) (Rodríguez-González et al., 2014, Gomes Marques et al., 2018).

The Ticino study site is located in the Lonate-Pozzolo basin within the Ticino regional Park (northern Italy), in a flat area close to the Ticino river (8°49′E, 45°26′N, 115 m a.s.l.). This area is part of the upper Po sub-basin, which has been regulated at least for the past 60 years (Colangelo et al., 2018). Climate in the study area is temperate and humid. Mean annual precipitation is 1030 mm mainly concentrated in autumn with the highest and lowest values in October (122 mm) and January (59 mm), respectively. Whilst mean annual temperature is 12.6 °C, the coldest and warmest months are in January (0.8 °C) and July (24.6 °C), respectively. The site is characterized by the presence of the highly-permeable Upper Po Plain shallow aquifer, which is constituted by gravel and sand deposits over discontinuous clay layers located at least 50 m below the land surface. The substrate is dominated by sandy loam soils. The study site is a floodplain forest with mixed stands of oaks (*Quercus robur* L. and *Quercus petraea* Liebl.), *A. glutinosa* and *U. minor*. Some areas are dominated by invasive species such as black locust (*Robinia pseudoacacia* L.) (Colangelo et al., 2018).

2.2. Climate, drought and hydrological data

To obtain homogenised, long-term series of monthly climatic data (mean temperature, total precipitation) we used the European 0.25°-gridded E-OBS-v13.1 dataset (Cornes et al., 2018), and downloaded the corresponding series from the nearest 0.25° grid point located near each study site. To illustrate the site dryness, we calculated the annual average climatic moisture index (CMI) following Willmott and Feddema

(1992):

$$\mathrm{CMI} = \begin{cases} \frac{P}{PET} - 1, & if\ P < PET \\ 0, & if\ P = PET \\ 1 - \frac{P}{PET}, & if\ P > PET \end{cases} \quad (1)$$

where P and PET are the precipitation and potential evapotranspiration, respectively. The CMI ranges from −1 to +1, with higher values corresponding to wetter sites. The PET was calculated using the Hargreaves method (Hargreaves and Samani, 1982).

We also used the Standardized Precipitation Evapotranspiration Index (SPEI) to characterize drought severity (Vicente-Serrano et al., 2010). This multiscalar drought index was calculated for several timescales (from 1 to 24 months) to take into account the duration of water shortage. The SPEI varies from −3 to 3, being categorized as extremely wet (2.00 and above), very wet (1.50–1.99), moderately wet (1.00–1.49), near normal (−0.99 to 0.99), moderately dry (−1.00 to −1.49), severely dry (−1.50 to −1.99), and extremely dry (−2.00 and less) conditions. The SPEI was estimated using the SPEI package for R (Beguería and Vicente-Serrano, 2017).

Long-term annual discharge data were only available for the two Spanish sites located in the Ebro basin (Tudela and Zaragoza) and for the Portuguese site located at the Odelouca river. We obtained annual discharge data for the hydrological year (prior October to current September) for the period 1970–2016 from the National flow and discharge database (Centro de Estudios y Experimentación de Obras Públicas, https://ceh.cedex.es). Flow data were obtained from two gauging stations located in Castejón (42°11′N, 1°41′W, 260 m a.s.l.) and Santiago (41°39′N, 0°53″W, 201 m a.s.l.) bridges over the Ebro river and located 10.4 km and 6.2 km upstream and downstream from the Tudela and Zaragoza sites, respectively. Hydrological data from the Odelouca river were obtained from Portuguese Environmental Agency online database (http://snirh.pt). Monthly flow (Hm^3) records (1961–2000), were collected from Monte dos Pachecos gauging station (code 30G/01H, 37°18′N, 8°28′W, 55 m a.s.l.), located few meters downstream the river reach where the trees were sampled.

2.3. Field sampling and dendrochronological data

Field sampling included the measurement of tree diameter at breast height (Dbh, 1.3 m) and coring of dominant trees. We selected and sampled from 12 to 17 trees per site (Table 2). Two increment cores per tree were sampled per tree at 1.3 m using 5-mm Pressler increment borer. Tree rings were visually cross-dated and tree-ring widths were measured to the nearest 0.01 mm using a binocular microscope coupled to a computer with the LINTAB-TSAP package (Rinntech, Heidelberg, Germany). The COFECHA program was used to evaluate the visual cross-dating of tree-ring series (Holmes, 1983). Tree age at 1.3 m was estimated as the maximum number of rings of the two cross-dated radii per tree and considering only those cores showing the pith or curved innermost rings. To quantify growth, tree-ring widths were transformed into basal-area increment (BAI) assuming concentric rings and using the following formula:

$$BAI_t = \pi(R_t^2 - R_{t-1}^2) \quad (2)$$

where R is the radius of the tree and t is the year of tree–ring formation.

We developed site mean series of ring-width indices (chronologies) for the five sites using the *dplR* (Bunn, 2010, Bunn et al., 2018) and *detrendeR* R packages (Campelo et al., 2012). We fitted 30-year long smoothing splines with a response of 0.5 to each tree-ring width series. Then, auto-regressive models were applied to each indexed ring-index series. The resulting individual series were averaged using bi-weight robust means to compute the pre-whitened, residual chronology in each site (Fritts, 1976).

Several dendrochronological statistics were calculated on each chronology to compare them (Briffa and Jones, 1990): AR1, first-order autocorrelation of raw ring-width data measuring the temporal persistence of growth; Ms, mean sensitivity of ring-width indices measuring the relative changes in width between consecutive rings; Rbar, mean inter-series correlations, measuring the internal coherence between individual series within each site. Lastly, we calculated the Expressed Population Signal (EPS) to assess how similar the chronologies were to a theoretical, infinitely replicated chronology (Wigley et al., 1984). Following these authors, and considering an EPS value higher than of 0.85, we determined the best replicated period for each chronology.

2.4. Statistical analyses

2.4.1. Site-level approach

We analysed how climate and tree features were related to radial growth using two approaches, at the site and individual level, and considering site series of ring-width indices and individual BAI data, respectively. First, we compared Dbh, tree age and mean tree-ring width between sites using Mann-Whitney tests. Second, to assess climate- and drought-growth relationships we used Pearson correlations and related site chronologies with the corresponding monthly climate data (mean temperature, total precipitation). Correlations were calculated for the best-replicated and common period 1970–2009 considering monthly or seasonal climate data. These analyses were performed from previous September in the year before the tree-ring was formed to September of the year of tree-ring formation (hydrological year). In the case of the SPEI, we calculated correlations considering 1- to 24-month SPEI values based on previous analyses in other Mediterranean tree species (Gomes Marques et al., 2018, Pasho et al., 2011). Lastly, we calculated correlations between the monthly annual discharge of the Ebro river and the Tudela and Zaragoza chronologies and between the monthly and annual flows of the Odelouca river and the Odelouca chronology. Climate- and drought-growth correlations were calculated using the *treeclim* R package (Zang and Biondi, 2015).

2.4.2. Individual-level approach

First, linear mixed effects models (LMMs) were fitted to investigate the relationships between BAI and seasonal climate variables at the individual tree level. In particular, seasonal values of temperature and precipitation of December-January-February (DJF), March-April-May

Table 2
Trees' features, tree-ring width data and dendrochronological statistics calculated for the common, best-replicated period 1970–2009. Values are means ± SD. Abbreviations: Dbh, diameter at breast height; AR1, First-order autocorrelation; Ms, Mean Sensitivity, Rbar, mean inter-series correlation; EPS, Expressed Population Signal. The Rbar and the EPS values were calculated using residual-series for the best-replicated period (1970–2009). The whole time span was taken for the ring-width statistics. Comparisons between sites were based on Mann-Whitney tests (different letters indicate significant differences, $p < 0.05$).

Site	No. trees (No. cores)	Dbh (cm)	Age at 1.3 m (years)	Tree-ring width (mm)	AR1	MS	Rbar	EPS	Period (EPS > 0.85)
Odelouca	12 (24)	46.0 ± 3.0b	62 ± 13b	3.97 ± 0.91b	0.62	0.37	0.32	0.83	1953–2009
Doñana	12 (23)	30.0 ± 1.2a	61 ± 12b	2.18 ± 0.41a	0.71	0.31	0.36	0.87	1947–2014
Zaragoza	14 (24)	34.0 ± 1.2a	46 ± 3a	2.85 ± 0.55ab	0.67	0.34	0.56	0.95	1969–2016
Tudela	17 (26)	31.0 ± 2.0a	47 ± 12a	2.77 ± 0.43ab	0.63	0.33	0.26	0.86	1970–2016
Ticino	16 (23)	36.0 ± 1.4a	59 ± 14a	3.21 ± 0.74b	0.66	0.27	0.21	0.80	1969–2017

(MAM), June-July-August (JJA), and September-October-November (SON) were treated as fixed effects. To account for the size- and age-related changes in tree growth, size (Dbh annual increment) and age (years) were incorporated as fixed effects. The models also included tree ID as well as its interaction with age (random slope) as random effects.

We used a top-down strategy to obtain the minimal model, starting with the model that contains all fixed explanatory variables. All explanatory variables were centred to prevent collinearity between main effects and increase parameter interpretability (Schielzeth, 2010). The parameters of fixed structure in the equations were estimated by maximum likelihood (ML), whilst the restricted maximum likelihood (REML) estimators was used to estimate the random components of the model (Pinheiro and Bates, 2000). The likelihood ratio test was used for testing the statistical significance of random effects in LMMs and to determine the appropriate variance function and autoregressive structure (Pinheiro and Bates, 2000).

Models reduction was performed throughout a stepwise approach which selected the most parsimonious model by minimizing the corrected Akaike Information Criterion (AICc). At the end the reduced model gave the smallest goodness-of-fit indicators, i.e. lowest values of AICc and Bayesian information criterion (BIC) (Burnham and Anderson, 2002). The variance inflation factor (VIF) was computed on the reduced models in order to test multicollinearity: the threshold for rejecting alternatives was 2 since VIF $>$ 2 suggested redundant explanatory variables (Dormann et al., 2013).

Inspection of the model fits suggested that the variance of the within-tree residuals increased with increasing expected BAI values, suggesting variance heterogeneity in the data. Then a variance structure component that allows specification of model variance heterogeneity of the within-group (Pinheiro and Bates, 2000) was also accounted to correct mis-specifications of the basic models. Additionally, the autocorrelation-moving average correlation structure corARMA of order (p, q) was used to address the within-tree autocorrelations of the errors observed in the data. Marginal R^2 values (Nakagawa and Schielzeth, 2013) were computed using the *r.squared* function of the R package *MuMIn* (Barton, 2020). We obtained the marginal (R^2_m) and conditional R^2 values (R^2_c) accounting for the variance explained by fixed and fixed plus random effects, respectively. All statistical computations were implemented in R (R Development Core Team, 2020), and parameter estimation was carried out by using the *nlme* library (Pinheiro and Bates, 2000).

3. Results

3.1. Tree and growth features

In terms of tree features and mean population characteristics, the Odelouca, Ticino and Doñana sites showed the oldest trees reaching maximum ages at 1.3 m of 106, 100 and 93 years, respectively. In the two sites from the Ebro basin, trees were younger with maximum ages of 77 and 53 years in Tudela and Zaragoza, respectively. Mean ages were significantly ($p < 0.05$) higher in Odelouca and Doñana than elsewhere (Table 2). In Odelouca, the largest diameters at breast height were recorded (mean Dbh = 46.0 cm), being also the site with the largest average growth rate (3.97 mm) among the studied sites. On the other extreme, Doñana showed the smallest growth rate (2.18 mm). Both Odelouca and Ticino study sites showed a higher variability in the tree-ring width standard deviation, whereas the first-order autocorrelation was highest in Doñana and Zaragoza. The mean sensitivity was low in Ticino (0.27), with a global average value of 0.32 indicating moderate year-to-year growth variability. The series intercorrelation peaked in Zaragoza with a value of 0.59 suggesting a high internal coherence in response to external drivers (e.g. climate or hydrological variables). Accordingly, the Expressed Population Signal was highest for Zaragoza (0.89), while Ticino (0.67) and Odelouca (0.68) showed the lowest values. The common and best-replicated period was 1970–2009 (Fig. 2) with EPS values greater than 0.85.

When comparing the chronologies using Pearson correlations, we found significant associations for the sites from south-western (Odelouca and Doñana, $r = 0.67$, $p = 0.001$) and north-eastern Iberia (Tudela and Zaragoza, $r = 0.46$, $p = 0.003$) indicating common growth variability in these two climatically contrasting regions (Figs. 1 and 2).

3.2. Growth responses to tree level features and climate

The selected LMMs showed that tree Dbh was the most important predictor of BAI, except in Ticino where tree age was more important (Table 3). The models showed a high explanatory power with fixed factors explaining from 28% (Doñana, Tudela) to 63% (Ticino) of BAI variance. In general, warm spring (March to May) conditions negatively impacted radial growth for the three dry sites (Doñana, Tudela and Zaragoza). On the other hand, both the prior winter (December to

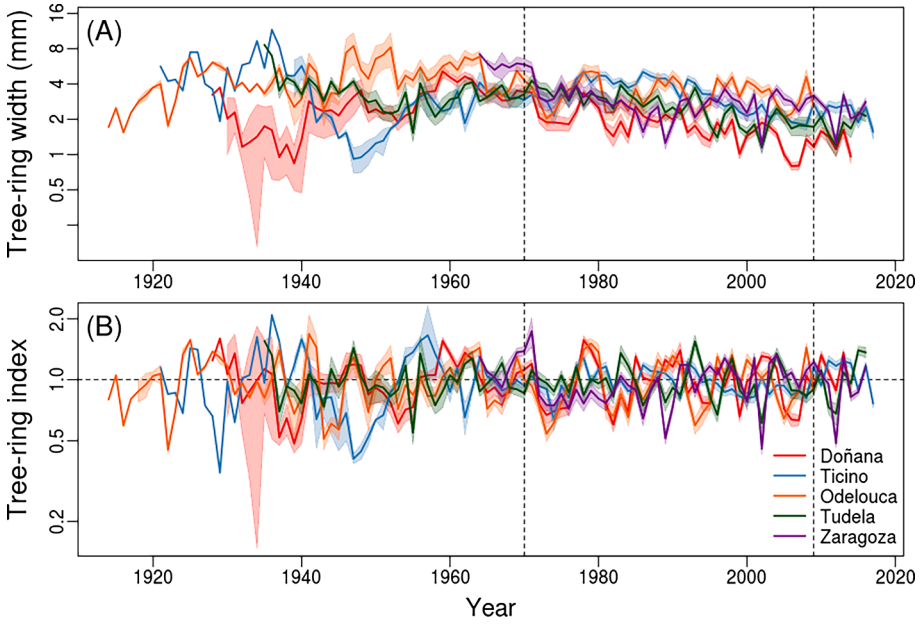

Fig. 2. Mean series of tree-ring width, where y values are log means ± SE (a) and ring-width indices where y values are means ± SE (b) of the five study sites. Vertical lines indicate beginning and end of best replicated period with higher EPS (1970–2009).

Table 3
Standardized estimates of the selected linear mixed-effects models fitted to annual radial growth (basal area increment) data as a function of seasonal climate variables, tree age and diameter at breast height (Dbh) in the five study sites. Numbers within parentheses are the standard errors of the estimates. Previous and current-year months are abbreviated with lowercase and uppercase letters, respectively. Seasons are abbreviated as follows: son, previous autumn (son, September to November); winter (dJF, previous December up to current February); and current spring (MAM, March to May) and summer (JJA, June to August). The last four rows show the statistics of the models including the R^2_m and R^2_c, which correspond to the marginal and conditional R^2 values accounting for the variance explained by fixed and fixed plus random effects, respectively. Significance levels: $^*p \leq 0.05$, $^{**}p < 0.01$, $^{***}p < 0.001$.

Climate variable	Season	Odelouca	Doñana	Tudela	Zaragoza	Ticino
Temperature	son					0.01 (0.01)
	dJF		0.02 (0.01)			−0.03 (0.01)
	MAM	0.04 (0.02)	−0.12** (0.02)	−0.07** (0.01)	−0.07** (0.01)	
	JJA		0.004 (0.01)			−0.16** (0.02)
Precipitation	son		−0.01 (0.01)		−0.07** (0.01)	−0.05** (0.01)
	dJF	0.08** (0.01)	0.05** (0.01)		0.07** (0.01)	
	MAM	0.10** (0.01)	0.07** (0.01)		−0.007 (0.01)	
Age		0.14* (0.06)	0.06 (0.06)	0.19** (0.07)	0.24** (0.04)	0.52** (0.07)
Dbh		0.67** (0.08)	0.51** (0.06)	0.32** (0.05)	0.44** (0.05)	0.41** (0.06)
R^2_m		0.40	0.28	0.28	0.53	0.63
R^2_c		0.50	0.30	0.56	0.56	0.85
AICc		20841.55	19205.13	18551.75	17665.88	16864.06
BIC		20931.78	19312.67	18749.31	17881.25	17072.39

February) precipitation and the current spring (March to May) precipitation showed a significant positive effect on growth in Odelouca and Doñana. In Zaragoza, growth decreased as prior autumn (September to November) precipitation increased. However, growth increased when prior winter conditions were wet, similarly to Doñana and Odelouca sites. In Ticino, growth decreased in response to warm summer and wet prior autumn conditions.

3.3. Growth responses to climate and drought at the site level

Correlations of climatic variables with ring-width indices in the five ash sites were generally consistent with the modelling results, especially for precipitation (Fig. 3, Suppl Mat 1). Specifically, correlations showed a significant positive relationship of prior winter and current spring precipitation with the Odelouca and Doñana chronologies, and a positive significant correlation with previous November precipitation. In Tudela and Zaragoza, a prior wet autumn increased growth, whilst warm-wet conditions in the prior November and a warm December also enhanced it in Tudela. In Zaragoza and Ticino, a wet prior-October was associated to wider rings. In Ticino, wet conditions associated to mild temperatures in July or summer enhanced growth. High spring precipitation was also associated to higher growth.

In terms of growth responses to drought (SPEI), the highest correlations and longest response periods were found in Odelouca (maximum $r = 0.62$, $r > 0.55$ from April to August at 6- to 14-month SPEI resolutions) and Doñana (maximum $r = 0.59$, $r > 0.55$ from April to July at 7- to 13-month SPEI resolutions), while Tudela and Zaragoza showed lower correlations (Tudela, $r = 0.39$; Zaragoza, $r = 0.40$), in the early growing season or before (January to April) and at shorter SPEI timescales (4–9 months) (Fig. 4). The climatically wettest Ticino site exhibited a significant positive correlation of ring-width index with the July SPEI ($r = 0.55$) at short to mid resolutions (2–10 months).

3.4. Relationships between growth and hydrology at the site level in the Ebro and Odelouca rivers

The Tudela chronology showed positive and significant ($p < 0.05$) correlations with previous winter (December and February), but also with summer (June, July) and autumn (September) monthly flow values (Fig. 5a). The highest correlations were found for March ($r = 0.49$, $p = 0.003$) and August ($r = 0.39$, $p = 0.007$). In the driest Zaragoza site (cf. Table 1 and Fig. 1), correlations were only significant for winter months, specifically December ($r = 0.32$, $p = 0.03$) and January ($r = 0.35$, $p = 0.01$). The river discharges peaked in the transition from winter to spring (Fig. 5a). The annual flow of the Ebro river was significantly and positively correlated with the Tudela ($r = 0.44$, $p = 0.002$) and Zaragoza ($r = 0.49$, $p = 0.001$) chronologies (Fig. 5b). However, there were evident outliers in the Tudela scatter plot with years such as (e.g., 1978–1979) showing very high discharges (13,010 Hm^3) but narrow rings (mean ring-width index 0.78), and years (e.g., 2014–2015) with moderate discharges (8875 Hm^3) and very wide rings (mean ring-width index 1.72).

In the Odelouca river the chronology showed positive and significant ($p < 0.05$) correlations in the monthly flow values of prior winter (November to February), but also from April to July (Fig. 6a). The highest correlations were found for prior December ($r = 0.64$, $p = 0.0001$), also when monthly river flow peaks (Fig. 6a). The annual flow of the Odelouca river was significantly and positively correlated with the study site chronology ($r = 0.78$, $p = 0.0001$) (Fig. 6b). The maximum annual flow corresponded to hydrologic year 1995–1996 (632.683 Hm^3), when the widest rings in this site were formed (mean ring-width index 1.49), whilst the lowest values (4.11 Hm^3) corresponded to the hydrologic year 1980–1981, when narrowest rings were formed (mean ring-width index 0.63).

4. Discussion

As hypothesized, we found that the growth responses to drought (SPEI) of the riparian narrow-leaved ash were stronger in the warmest-driest sites (Doñana and Odelouca, with CMI −0.60 and −0.43, respectively), in terms of climate water balance (CMI), but contrary to expected those responses did not peak in the driest sites (Tudela and Zaragoza, with lowest values of annual precipitation). In the wettest and coolest site (Ticino), the growth response to drought was also notable but peaked in summer suggesting a unimodal growth pattern with delayed cambial phenology. The growth responses to drought peaked in spring in the warmest-driest sites and lasted longer (6 to 14 months), suggesting longer growing seasons. However, in the semi-arid Mediterranean continental sites from the Ebro basin (Tudela and Zaragoza), the growth response to drought peaked in the transition from winter to spring and was of moderate duration (from 4 to 9 months). Interestingly, this response is similar to tree species response from dry or semi-arid nearby sites as Aleppo pine (*Pinus halepensis* Mill.) whose growth depends on prior winter precipitation that recharges soil moisture depleted in late summer (Pasho et al., 2011). This response agrees with functional and morphological traits of ash species (e.g., root system), which can

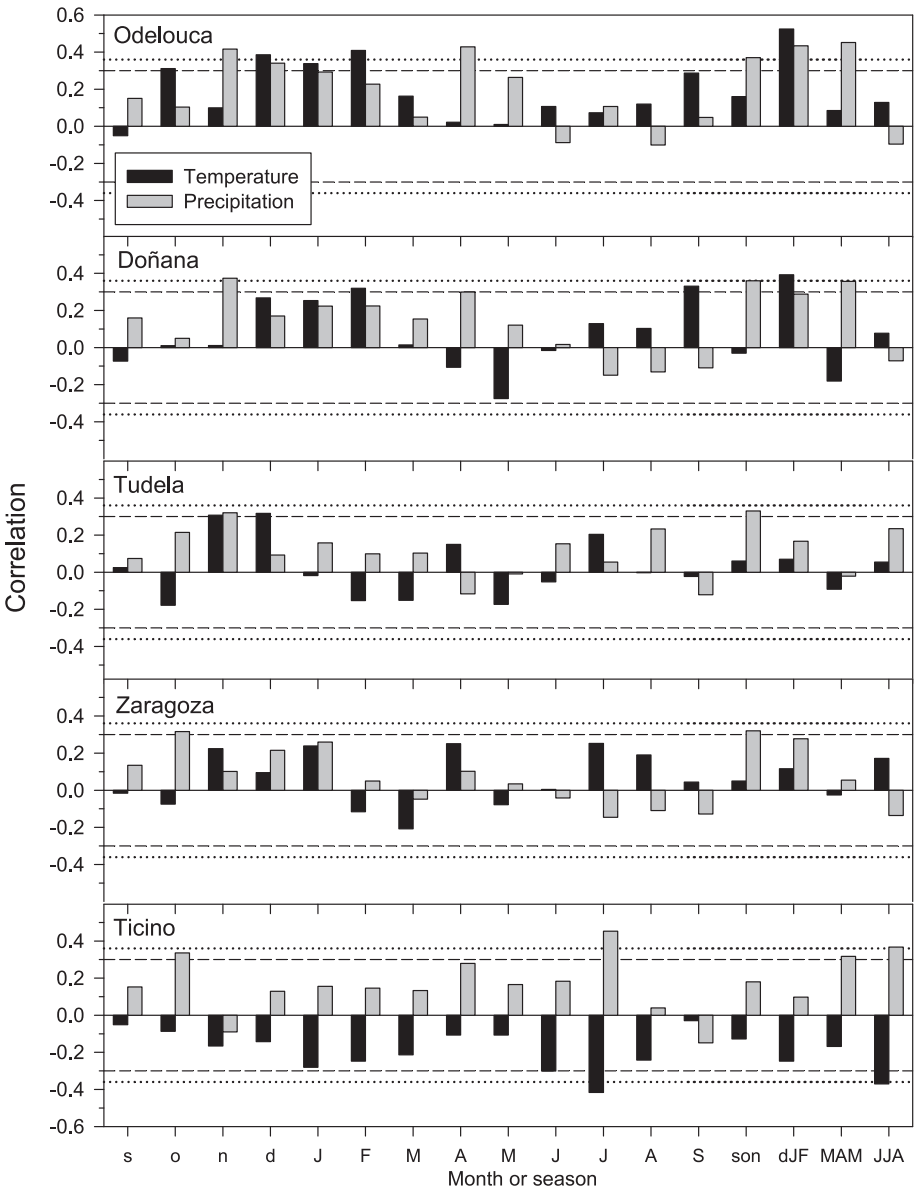

Fig. 3. Relationships between climate and ring-width indices developed for the five study sites for the common period (1970–2009). Bars show Pearson correlations calculated between seasonal and monthly climate variables (mean temperature and total precipitation) and mean series of ring-width indices. Correlations were calculated from prior to current September (months abbreviated by lowercase letters correspond to the year prior to tree-ring formation). Dashed and dotted horizontal lines show the 0.05 and 0.01 significance levels, respectively.

explain a coupling to hydroclimate conditions and reduced growth responses to groundwater variations (Dufour and Piégay, 2008). Nevertheless, the long-term discharge data available for these two sites of the Ebro basin and also for the Odelouca site illustrated that narrow-leaved ash growth positively responded to monthly flow during the flow peak, from December to March, which allows replenishing shallow soil water reserves of these riparian forests. Interestingly, the responses were stronger in Tudela and Odelouca than in Zaragoza and extended to the late growing season (summer and early autumn) in the first site and to the early growing season in Odelouca (spring and early summer). These findings indicate that Tudela and Odelouca trees are better coupled with the river hydrological regime than Zaragoza individuals, a pattern observed in other riparian trees in Mediterranean regions, such as *Populus trichocarpa*, in California (Stromberg and Patten, 1996). It also agrees with the better conservation status (free-flowing not affected by regulation) of the fluvial reaches harbouring both Tudela floodplain forests (Ayerra, 1988; Ollero, 1990, González et al., 2012) and Odelouca riparian forests (Rodríguez-González et al., 2014). Furthermore, these results are consistent with a study from two rivers in central Spain where narrow-leaved ash growth was found to be favoured by spring and summer river flow (González Muñoz et al., 2015).

The findings reported agree with our current knowledge on ash species phenology such as common ash, whose first earlywood vessels start to enlarge before budburst and cambial division resumes after budburst (Funada and Catesson, 1991; Frankenstein et al., 2005; Sass-Klaassen et al., 2011; Klesse et al., 2020). In another Mediterranean ash species, the manna ash (*Fraxinus ornus* L.), cambial cell production started in early March, before buds were swollen, and ceased in mid-July (Gričar et al., 2020). Our climate- and drought-growth correlation analyses suggest that in Ticino, the wettest and coolest site, the high rates of latewood produced in July point to a unimodal growth pattern. On the other hand, in the warmest sites of Odelouca and Doñana the peak growth rates were reached in April, with the possibility of a minor peak (bimodal growth pattern) after the summer (Camarero et al. 2010, Campelo et al. 2018). In Odelouca, the growth peak near the vernal equinox could be a safety mechanism to ensure low growth rates during the summer drought (Vieira et al. 2020), while the maximum growth rates around the summer solstice in Ticino could be to take full advantage of the long days and water availability. In both cases, these growth rates would be controlled by soil water availability and drought indicating a plastic phenology of the narrow-leaved ash across its distribution range, regardless of the different hydrological settings which were

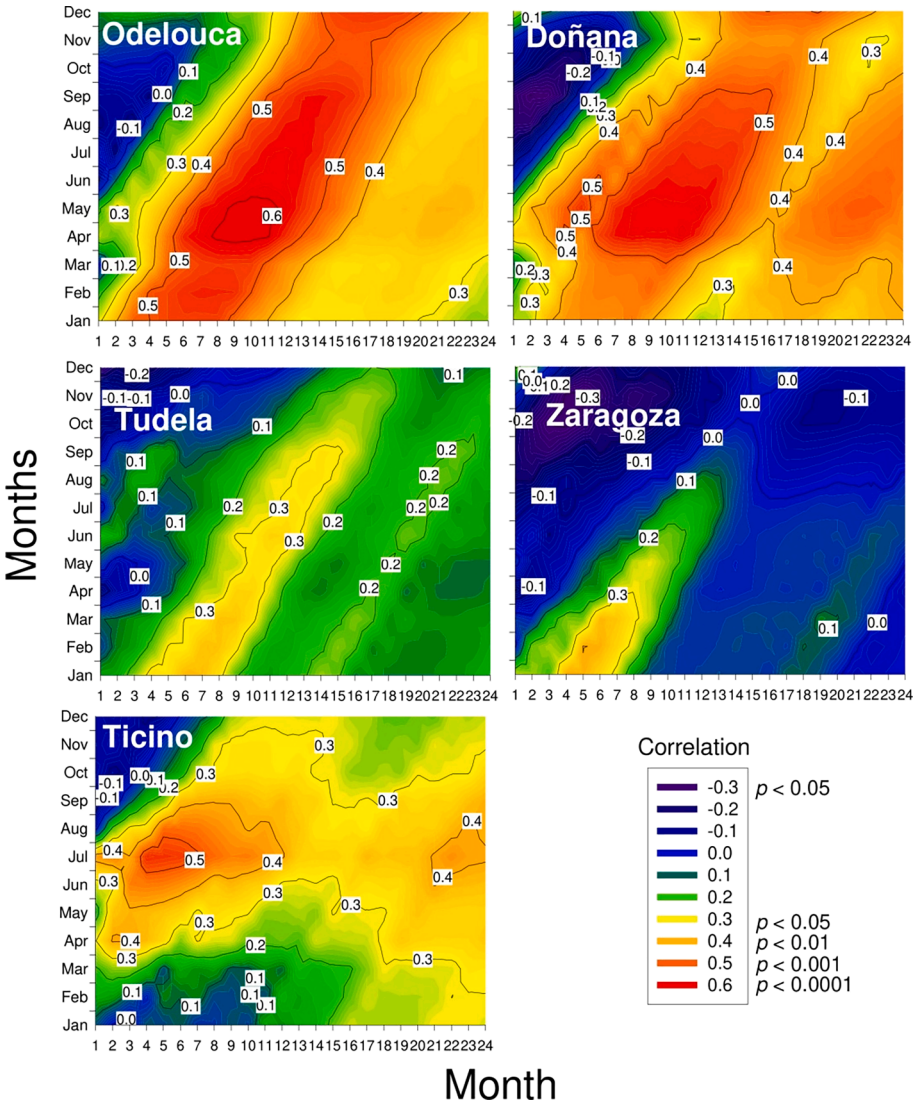

Fig. 4. Correlations calculated between monthly SPEI values and mean series of ash ring-width indices for the five study sites considering 1–24 monthly resolution (x axes) and months of the growth year (y axes). The significance levels are shown near the color scale.

considered in this study. In the Ebro river sites, growth was highly correlated to prior winter precipitation causing a mid-term response to early growing-season droughts. This indicates a stronger coupling to regional climate conditions, which was buffered in the Tudela site where growth responds to changes in the winter river discharge. Nonetheless, the outliers in the scatter between annual discharge and ring-width indices observed when plotting Tudela data indicate that growth was also uncoupled from the river hydrological regime, perhaps because of local microclimate conditions or biotic interactions, including pests or defoliators, which can depend on the flood regime (Verheyde and Sioen, 2019). The Ebro river is regulated since the 1960s (González et al., 2012), so growth-discharge uncoupling could be linked to site factors since they were not observed in the Zaragoza site, despite both Tudela and Zaragoza sites are similarly impacted by regulation of the hydrological regime. Remarkably, the youngest trees were found in the Zaragoza site, confirming its higher local anthropogenic disturbance intensity related to several land-use drivers affecting European rivers (urban expansion, agricultural conversion, building of local river breakwaters; see Belletti et al., 2020). In the study sites, ash trees competed with other species (poplars, oaks, alder, elm) and in some sites, as Zaragoza and Tudela, coexisted with young elm trees affected by Dutch elm disease (J.J. Camarero, *pers. observ.*). In this regard, the analyses at the individual level emphasized the effect of tree size on growth rates, albeit we missed relevant local information such as competition with neighbouring trees, microtopography, soil depth or distance to the active river channel (Rodríguez-González et al., 2017). For example, the absence of regular floods has been reported to benefit upland species, which may outcompete ash in more shaded and dense stands (Janík et al., 2016). On the other hand, channel-floodplain anthropic disconnections could make ash more drought sensitive and dependent on local precipitation. In addition, individual- and site-level analyses showed opposite results in some case as the associations between prior autumn conditions and growth in Zaragoza. This could be due to the use of different responses variables (BAI vs. ring-width indices) or to the strengthening of some climate signals when averaging individual series and using mean site series (chronologies). Our individual-level analyses also illustrated the relevance of cool-wet conditions in the prior winter and current spring as positive drivers of radial growth in most sites, except the wettest Ticino floodplain forest. Finally, some features of ash radial growth such as vessel size have been found, in other regions, to depend on other climate factors than precipitation such as prior winter temperatures (Zhu et al., 2020), pointing out for the need of further research, incorporating anatomical traits in studies about Mediterranean narrow-leaved ash populations.

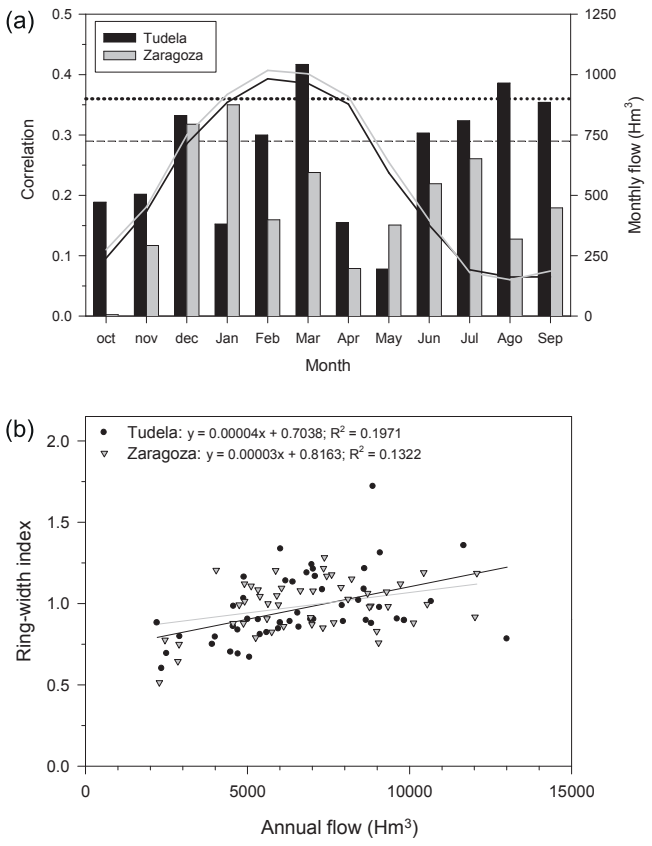

Fig. 5. The chronologies (mean site ring-width series) of narrow-leaved ash from Tudela and Zaragoza sites were positively related to the monthly (a) and annual (b) flow of the Ebro river. In the plot (a) bars are Pearson correlations and the lines indicate the monthly flows flows (right *y* axis). Months of the previous and current years are abbreviated by lowercase and uppercase letters, respectively. Dashed and dotted horizontal lines show the 0.05 and 0.01 significance levels, respectively. In the plot (b) the period 1970–2016 with available hydrologic data is plotted and different lines correspond to different sites.

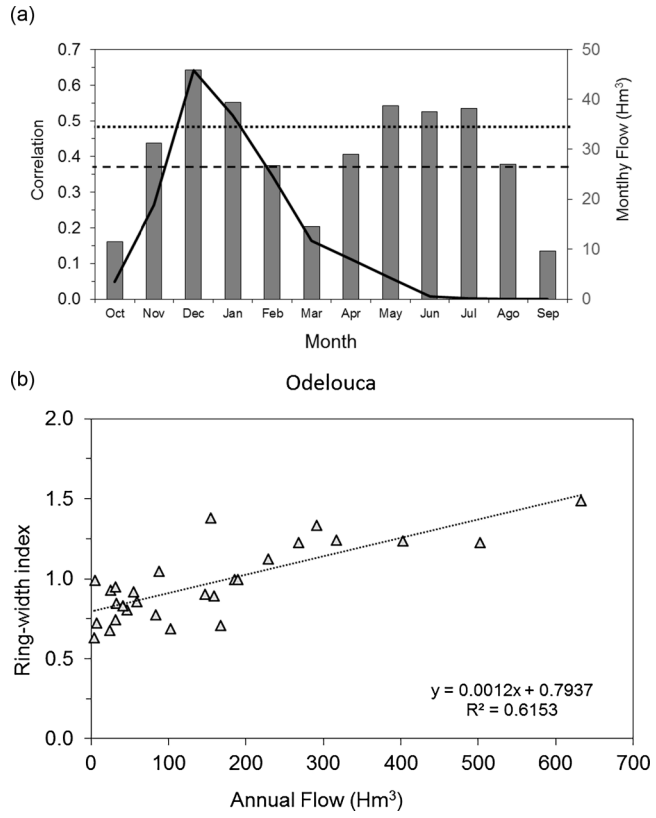

Fig. 6. The chronologies (mean site ring-width series) of narrow-leaved ash from the Odelouca site were positively related to the monthly (a) and annual (b) flow of the Odelouca river. In the plot (a) bars are Pearson correlations and the lines indicate the monthly discharges (right *y* axis). Months of the previous and current years are abbreviated by lowercase and uppercase letters, respectively. Dashed and dotted horizontal lines show the 0.05 and 0.01 significance levels, respectively. In the plot (b) the period 1970–2000 with available hydrologic data is plotted.

4.1. Management implications for Mediterranean riparian forests

Mediterranean floodplain forests are endangered habitats with a great ecological importance showing high biodiversity levels and providing multiple ecosystem services (improving water quality, mitigating flood effects, formation of fertile soils, etc.), far beyond the land area they occupy. These make floodplain forests of high conservation priority in Europe (European Commission, 2013), yet their conservation status is unfavourable to bad, particularly in the Mediterranean Region (EEA, 2015)

The narrow-leaved ash is dominant ash in floodplains of the Mediterranean basin, with a relatively large ecological spectrum from active channel to floodplain, to terrace, and from wetland (i.e. lentic) to river (i.e. lotic) habitats; thus, it is a potentially very appealing species for conservation and restoration actions in the context of climate change as a foundation species modulating recovery of the riparian ecosystem. However, our results indicate that ongoing global warming could impose additional growth reduction and threaten the survival of some narrow-leaved ash stands notably those located in dry, warm sites. Given the projected warming and drying trends and more intense pressure on hydric resources in the Mediterranean Basin (García-Ruiz et al., 2011), these riparian forests should be protected, managed or restored considering their increasing coupling to regional climate conditions but uncoupling from altered hydrological regimes (this study). Our findings provide ecological information on *Fraxinus angustifolia* requirements, necessary considerations in either a passive restoration approach based in promoting ecological processes for allowing natural recovery (Beechie et al., 2010), or in active strategies which should project spatial distribution of riparian species across the riverbank topographic gradient (Magdaleno et al., 2014), as potential distribution shifts may be expected in a context of increased aridification (Gomes Marques et al., 2018).

Projected climate aridification (García-Ruiz et al., 2011) and hydrological alteration (Belletti et al., 2020) will increase vulnerability as a result of interaction with several biotic threats affecting forests worldwide. For example, impairment of the natural flow regime has been related with ash decline in alluvial forests (Janík et al., 2016), and this effect may be exacerbated by competitive pressure by biological invasions (Nadal-Sala et al., 2017). Also, hydroclimatic stress may intensify impact of emerging diseases affecting ash species (Adamcikova et al., 2018), with implications at the ecosystem level. In order to properly include these multiple stressors into restoration programmes (Johnson et al., 2020), future research should integrate biotic and abiotic stressors effect (Stella et al., 2019) such as tree-growth and water-user performance interactions with biological pressures.

5. Conclusions

To conclude, we found diverse growth responses to climate and drought across the Mediterranean distribution range of the narrow-leaved ash. Overall, growth of this species increased in response to wet and cool conditions in the prior winter, and during the growing

season. The growth loss in response to drought peaked from prior winter up to summer and at short to long time resolutions indicating plastic responses to local site conditions. Hydrological conditions influenced the narrow-leaved ash with high river discharge or flow in the prior winter and early spring enhancing radial growth.

CRediT authorship contribution statement

Patricia M. Rodríguez-González: Conceptualization, Formal analysis, Funding acquisition, Investigation, Methodology, Resources, Writing - original draft, Writing - review & editing. **Michele Colangelo:** Investigation, Methodology, Writing - review & editing. **Ángela Sánchez-Miranda:** Investigation, Writing - review & editing. **Raúl Sánchez-Salguero:** Investigation, Writing - review & editing. **Filipe Campelo:** Formal analysis, Investigation, Methodology, Writing - review & editing. **Angelo Rita:** Formal analysis, Investigation, Methodology, Writing - review & editing. **Inês Gomes Marques:** Investigation, Writing - review & editing. **António Albuquerque:** Investigation, Writing - review & editing. **Francesco Ripullone:** Investigation, Writing - review & editing. **J. Julio Camarero:** Conceptualization, Formal analysis, Funding acquisition, Investigation, Methodology, Resources, Writing - original draft, Writing - review & editing.

Declaration of Competing Interest

The authors declare that they have no known competing financial interests or personal relationships that could have appeared to influence the work reported in this paper.

Acknowledgements

We are grateful to Rui Rivaes for help during field work in Odelouca site. The authors would like to thank the Doñana Biological Reserve and Doñana Biological Station, especially Ricardo Díaz Delgado for logistics support. The authors also would like to thank the Administration of the Ticino Regional Park, especially Fulvio Caronni for the logistic support during the field work. This study was supported by the BBVA Foundation through project "Sed en el río: cómo el calentamiento climático y los cambios en la dinámica fluvial contribuyen al declive de los bosques de ribera (SED-IBER)" lead by JJC. PMRG was supported by Portuguese Foundation for Science and Technology (FCT), through FCT Investigator Program grant number IF/00059/2015, and CEF (UID/AGR/00239/2019 and UIDB/00239/2020). Field sampling in Odelouca site was supported by RIPFLOW project (IWRM ERA-net programme), and in Doñana site was supported by the "Programa de Acceso a la Infraestructura Científica y Tecnológica Singular" (ICTS-25-2010), project "Doñana wetland forests as sentinels of global change". JJC and RSS acknowledge the support of VULBOS project (UPO-1263216) from the ERDF funds Andalusia regional government 2014-2020.

Appendix A. Supplementary material

Supplementary data to this article can be found online at https://doi.org/10.1016/j.foreco.2021.119128.

References

Adamcikova, K., Pažitný, J., Pastirčáková, K., 2018. Individual resistance of *Fraxinus angustifolia* and *F. excelsior* clones to *Hymenoscyphus fraxineus*. J. Plant Protection Res. 58, 227–233.

Andersen, D.C., 2016. Climate, streamflow, and legacy effects on growth of riparian *Populus angustifolia* in the arid San Luis Valley, Colorado. J. Arid. Environ. 134, 104–121.

Ayerra, E., 1988. Los sotos de la ribera Tudelana. Servicio de Medio Ambiente del Gobierno de Navarra, Pamplona, Spain.

Beguería, S., Vicente-Serrano, S. M., 2017. SPEI: Calculation of the Standardised Precipitation-Evapotranspiration Index. R package, version 1.7.

Barton, K., 2020. Mu-MIn: Multi-model inference. http://R-Forge.R-project.org/projects/mumin/.

Beechie, T.J., Sear, D.A., Olden, J.D., Pess, G.R., Buffington, J.M., Moir, H., Roni, P., Pollock, M.M., 2010. Process-based principles for restoring river ecosystems. BioScience 60, 209–222.

Belletti, B., Garcia de Leaniz, C., Jones, J., Bizzi, S., Börger, L., Segura, G., Castelletti, A., van de Bund, W., Aarestrup, K., Barry, J., Belka, K., Berkhuysen, A., Birnie-Gauvin, K., Bussettini, M., Carolli, M., Consuegra, S., Dopico, E., Feierfeil, T., Fernández, S., Fernandez Garrido, P., Garcia-Vazquez, E., Garrido, S., Giannico, G., Gough, P., Jepsen, N., Jones, P.E., Kemp, P., Kerr, J., King, J., Łapińska, M., Lázaro, G., Lucas, M.C., Marcello, L., Martin, P., McGinnity, P., O'Hanley, J., Olivo del Amo, R., Parasiewicz, P., Pusch, M., Rincon, G., Rodriguez, C., Royte, J., Schneider, C.T., Tummers, J.S., Vallesi, S., Vowles, A., Verspoor, E., Wanningen, H., Wantzen, K.M., Wildman, L., Zalewski, M., 2020. More than one million barriers fragment Europe's rivers. Nature 588, 436–441.

Briffa, K.R., Jones, P.D., 1990. Basic chronology statistics and assessment. In: Cook, E.R., Kairiukstis, L.A. (Eds.), Methods of Dendrochronology: Applications in the Environmental Sciences. Kluwer Academic Publishers, Boston, pp. 137–152.

Bunn, A., 2010. Statistical and visual crossdating in R using the dplR library. Dendrochronologia 28, 251–258. https://doi.org/10.1016/j.dendro.2009.12.001.

Bunn, A., Korpela, M., Biondi, F., Campelo, F., Mérian, P., Qeadan, F., Zang, C., Pucha-Cofrep, D., Wernicke, J., 2018. dplR: Dendrochronology Program Library in R.R Package Version 1.6.8.

Burnham, K.P., Anderson, D.R., 2002. Model Selection and Multimodel Inference: A Practical Information-Theoretic Approach, second ed. Springer, Berlin.

Camarero, J.J.J., Olano, J.M., Parras, A., 2010. Plastic bimodal xylogenesis in conifers from continental Mediterranean climates. New Phytol. 185, 471–480. https://doi.org/10.1111/j.1469-8137.2009.03073.x.

Cailleret, M., Dakos, V., Jansen, S., Robert, E.M.R., Aakala, T., Amoroso, M.M., Antos, J. A., Bigler, C., Bugmann, H., Caccianaga, M., Camarero, J.J., Cherubini, P., Coyea, M. R., Čufar, K., Das, A.J., Davi, H., Gea-Izquierdo, G., Gillner, S., Haavik, L.J., Hartmann, H., Hereş, A.-M., Hultine, K.R., Janda, P., Kane, J.M., Kharuk, V.I., Kitzberger, T., Klein, T., Levanic, T., Linares, J.-C., Lombardi, F., Mäkinen, H., Mészáros, I., Metsaranta, J.M., Oberhuber, W., Papadopoulos, A., Petritan, A.M., Rohner, B., Sangüesa-Barreda, G., Smith, J.M., Stan, A.B., Stojanovic, D.B., Suarez, M.-L., Svoboda, M., Trotsiuk, V., Villalba, R., Westwood, A.R., Wyckoff, P.H., Martínez-Vilalta, J., 2019. Early-warning signals of individual tree mortality based on annual radial growth. Front. Plant Sci. 9, 1964.

Campelo, F., García-González, I., Nabais, C., 2012. detrendeR - A Graphical User Interface to process and visualize tree-ring data using R. Dendrochronologia 30, 57–60. https://doi.org/10.1016/j.dendro.2011.01.010.

Campelo, F., Gutiérrez, E., Ribas, M., Sánchez-Salguero, R., Nabais, C., Camarero, J.J., 2018. The facultative bimodal growth pattern in *Quercus ilex* – A simple model to predict sub-seasonal and inter-annual growth. Dendrochronologia 49, 77–88. https://doi.org/10.1016/j.dendro.2018.03.001.

Caudullo, G., Houston Durrant, T., 2016. Fraxinus angustifolia in Europe: distribution, habitat, usage and threats. In: San-Miguel-Ayanz, J., de Rigo, D., Caudullo, G., Houston Durrant, T., Mauri, A. (Eds.), European Atlas of Forest Tree Species. Publ. Off. EU, Luxembourg, pp. e0101d2.

Colangelo, M., Camarero, J.J., Ripullone, F., Gazol, A., Sánchez-Salguero, R., Oliva, J., Redondo, M.A., 2018. Drought decreases growth and increases mortality of coexisting native and introduced tree species in a temperate floodplain forest. Forests 9, 1–17. https://doi.org/10.3390/f9040205.

Cornes, R., van der Schrier, G., van den Besselaar, E.J.M., Jones, P.D., 2018. An ensemble version of the E-OBS temperature and precipitation datasets. J. Geophys. Res-Atmos. 123 https://doi.org/10.1029/2017JD028200.

Dormann, C.F., Elith, J., Bacher, S., Buchmann, C., Carl, G., Carré, G., Marquéz, J.R.G., Gruber, B., Lafourcade, B., Leitão, P.J., Münkemüller, T., McClean, C., Osborne, P.E., Reineking, B., Schröder, B., Skidmore, A.K., Zurell, D., Lautenbach, S., 2013. Collinearity: a review of methods to deal with it and a simulation study evaluating their performance. Ecography 36, 27–46.

Dufour, S., Piégay, H., 2008. Geomorphological controls of *Fraxinus excelsior* growth and regeneration in floodplain forests. Ecology 89, 205–215.

Dufour, S., Rodríguez-González, P.M., Laslier, M., 2018. Tracing the scientific trajectory of riparian vegetation studies: main topics, approaches and needs in a globally changing world. Sci. Total. Environ. 653, 1168–1185. https://doi.org/10.1016/j.scitotenv.2018.10.383.

European Environment Agency (EEA), 2015. Conservation status of habitat types and species (Article 17, Habitats Directive 92/43/EEC). (accessed 9 November 2020) https://www.eea.europa.eu/data-and-maps/daviz/conservation-status-of-floodplain-forest-habitats.

Enderle, R., Stenlid, J., Vasaitis, R., 2019. An overview of ash (*Fraxinus* spp.) and the ash dieback disease in Europe. CAB Rev. 14, 1–12.

European Commission, 2013. Interpretation manual of European Union Habitats–EUR26. European Commission DG Environment, Brussels, Belgium.

Frankenstein, C., Eckstein, D., Schmitt, U., 2005. The onset of cambium activity —a matter of agreement? Dendrochronologia 23, 57–62. https://doi.org/10.1016/j.dendro.2005.07.007.

Fritts, H., 1976. Tree Rings and Climate. Academic Press, London.

Frutos, L.M., Ollero, A., and Sánchez Fabre, M. 2004. Caracterización del Ebro y su cuenca y variaciones en su comportamiento hidrológico, in: Alteración de los regímenes fluviales peninsulares, edited by: Gil Olcina, A. (Coord.), Fundación Cajamurcia, Murcia, Spain, pp. 233–280.

Funada, R., Catesson, A.M., 1991. Partial cell wall lysis and the resumption of meristematic activity in *Fraxinus excelsior* cambium. IAWA Bull. 12, 439–444.

García-Ruiz, J.M., López-Moreno, J.I., Vicente-Serrano, S.M., Lasanta-Martínez, T., Beguería, S., 2011. Mediterranean water resources in a global change scenario. Earth-Sci. Rev. 105, 121–139.

Garssen, A.G., Verhoeven, J.T., Soons, M.B., 2014. Effects of climate-induced increases in summer drought on riparian plant species: a meta-analysis. Freshwater Biol. 59, 1052–1063.

Gomes Marques, I., Campelo, F., Rivaes, R., Albuquerque, A., Ferreira, M.T., Rodríguez-González, P.M., 2018. Tree rings reveal long-term changes in growth resilience in Southern European riparian forests. Dendrochronologia 52, 167–176. https://doi.org/10.1016/j.dendro.2018.10.009.

González, E., González-Sanchís, M., Comín, F.A., Muller, E., 2012. Hydrologic thresholds for riparian forest conservation in a regulated large Mediterranean River. River Res. Appl. 28, 71–80.

González Muñoz, N., Linares, J.C., Castro-Díez, P., Sass-Klaassen, U., 2015. Contrasting secondary growth and water use efficiency patterns in native and exotic trees co-occurring in inner Spain riparian forests. For. Sys. 24, e017.

Gričar, J., Vedenik, A., Skoberne, G., Hafner, P., Prislan, P., 2020. Timeline of leaf and cambial phenology in relation to development of initial conduits in xylem and phloem in three coexisting sub-Mediterranean deciduous tree Species. Forests 11, 1104. https://doi.org/10.3390/f11101104.

Hargreaves, G.H., Samani, Z.A., 1982. Estimating potential evapotranspiration. J. Irrig. Drain E-ASCE 108, 225–230.

Holmes, R., 1983. Computer-assisted quality control in tree-ring dating and measurement. Tree-Ring Bull. 43, 69–78.

Hultberg, T., Sandström, J., Felton, A., Öhman, K., Rönnberg, J., Witzell, J., Cleary, M., 2020. Ash dieback risks an extinction cascade. Biol. Conserv. 244, 108516 https://doi.org/10.1016/j.biocon.2020.108516.

Janík, D., Adam, D., Hort, L., Král, K., Šamonil, P., Unar, P., Vrška, T., 2016. Patterns of *Fraxinus angustifolia* in an alluvial old-growth forest after declines in flooding events. Eur. J. Forest Res. 135, 215–228.

Johnson, M.F., Thorne, C.R., Castro, J.M., Kondolf, G.M., Mazzacano, C.S., Rood, S.B., Westbrook, C., 2020. Biomic river restoration: a new focus for river management. River Res. Appl. 36, 3–12.

Klesse, S., von Arx, G., Gossner, M.M., Hug, C., Rigling, A., Queloz, V., 2020. Amplifying feedback loop between growth and wood anatomical characteristics of *Fraxinus excelsior* explains size-related susceptibility to ash dieback. Tree Physiol. https://doi.org/10.1093/treephys/tpaa091.

Manzano, M., Custodio, E., Mediavilla, C., Montes, C., 2005. Effects of localised intensive aquifer exploitation on the Doñana wetlands (SW Spain). In: Sahuquillo, A., Capilla, J., Martínez-Cortina, L., Sanchez Vila, X. (Eds.), Groundwater Intensive Use, International Association of Hydrogeologists, Selected Papers on Hydrogeology. Taylor & Francis, pp. 209–219.

Magdaleno, F., Blanco-Garrido, F., Bonada, N., Herrera-Gao, T., 2014. How are riparian plants distributed along the riverbank topographic gradient in Mediterranean rivers? Application to minimally altered river stretches in Southern Spain. Limnetica 33, 121–138.

Nadal-Sala, D., Sabaté, S., Sánchez-Costa, E., Poblador, S., Sabater, F., Gracia, C., 2017. Growth and water use performance of four co-occurring riparian tree species in a Mediterranean riparian forest. For. Ecol. Manage. 396, 132–142.

Nakagawa, S., Schielzeth, H., 2013. A general and simple method for obtaining R^2 from generalized linear mixed-effects models. Methods Ecol. Evol. 4, 133–142.

Ollero, A., 1990. Espacios naturales de ribera en el municipio de Zaragoza. Geographicalia 27, 121–136.

Ollero, A., 2007. Channel adjustments, floodplain changes and riparian ecosystems of the middle Ebro River: assessment and management. Int. J. Water Resour. D 23, 73–90.

Pasho, E., Camarero, J.J., de Luis, M., Vicente-Serrano, S.M., 2011. Impacts of drought at different time scales on forest growth across a wide climatic gradient in north-eastern Spain. Agr. Forest Meteorol. 151, 1800–1811.

Pinheiro, J.C., Bates, D.M., 2000. Mixed-effects Models in S and S-Plus. Springer, New York.

R Core Team, 2019. R: A language and environment for statistical computing. R Foundation for Statistical Computing, Vienna, Austria.

Rodríguez-González, P.M., Stella, J.C., Campelo, F., Ferreira, M.T., Albuquerque, A., 2010. Subsidy or stress? Tree structure and growth in wetland forests along a hydrological gradient in Southern Europe. For. Ecol. Manage. 259, 2015–2025. https://doi.org/10.1016/j.foreco.2010.02.012.

Rodríguez-González, P.M., Campelo, F., Albuquerque, A., Rivaes, R., Ferreira, T., Pereira, J.S., 2014. Sensitivity of black alder (*Alnus glutinosa* [L.] Gaertn.) growth to hydrological changes in wetland forests at the rear edge of the species distribution. Plant Ecol. 215, 233–245. https://doi.org/10.1007/s11258-013-0292-9.

Rodríguez-González, P.M., Albuquerque, A., Martínez-Almarza, M., Díaz-Delgado, R., 2017. Long-term monitoring for conservation management: lessons from a case study integrating remote sensing and field approaches in floodplain forests. J. Environ. Manage. 202, 392–402.

Rodríguez-González, P.M., Ferreira, M.T., Albuquerque, A., Espirito Santo, D., Ramil Rego, P., 2008. Spatial variation of wetland woods in the latitudinal transition to arid regions: a multiscale approach. J. Biogeogr. 35, 1498–1511.

Sass-Klaassen, U., Sabajo, C.R., den Ouden, J., 2011. Vessel formation in relation to leaf phenology in Pedunculate oak and European ash. Dendrochronologia 29, 171–175.

Schielzeth, H., 2010. Simple means to improve the interpretability of regression coefficients. Methods Ecol. Evol. 1, 103–113.

Scott, M.L., Lines, G.C., Auble, G.T., 2000. Channel incision and patterns of cottonwood stress and mortality along the Mojave River, California. J. Arid Environ. 44, 399–414.

Scott, M.L., Shafroth, P.B., Auble, G.T., 1999. Responses of riparian cottonwoods to alluvial water table declines. Environ. Manag. 23, 347–358.

Singer, M.B., Stella, J.C., Dufour, S., Piégay, H., Wilson, R.J., Johnstone, L., 2013. Contrasting water uptake and growth responses to drought in co-occurring riparian tree species. Ecohydrology 6, 402–412. https://doi.org/10.1002/eco.1283.

Stella, J.C., Bendix, J., 2019. Multiple stressors in riparian ecosystems. In: Multiple Stressors in River Ecosystems. Elsevier, pp. 81–110.

Stella, J.C., Riddle, J., Piegay, H., Gagnage, M., Tremelo, M.L., 2013. Climate and local geomorphic interactions drive patterns of riparian forest decline along a Mediterranean Basin river. Geomorphology 202, 101–114. https://doi.org/10.1016/j.geomorph.2013.01.013.

Stella, J.C., Bendix, J., 2019b. Multiple stressors in riparian ecosystems. In: Sabater, S., Elosegi, A., Ludwig, R. (Eds.), Multiple Stressors in River Ecosystems. Elsevier, pp. 81–110.

Stromberg, J.C., Patten, D.T., 1996. Instream flow and cottonwood growth in the eastern Sierra Nevada of California, USA. Regulated Rivers: Res. Manage. 12, 1–12.

Tulik, M., Grochowina, A., Jura-Morawiec, J., Bijak, S., 2020. Groundwater level fluctuations affect the mortality of black alder (*Alnus glutinosa* Gaertn.). Forests 11, 134. https://doi.org/10.3390/f11020134.

Valor, T., Camprodon, J., Buscarini, S., Casals, P., 2020. Drought-induced dieback of riparian black alder as revealed by tree rings and oxygen isotopes. For. Ecol. Manage. 478, 118500.

Verheyde, F., Sioen, G., 2019. Outbreaks of *Tomostethus nigritus* (Fabricius, 1804) (Hymenoptera, Tenthredinidae) on *Fraxinus angustifolia* 'Raywood' in Belgium. J. Hymenoptera Res. 72, 67–81. https://doi.org/10.3897/jhr.72.38284.

Vicente-Serrano, S.M., Beguería, S., López-Moreno, J.I., 2010. A multiscalar drought index sensitive to global warming: the standardized precipitation evapotranspiration index. J. Climate 23, 1696–1718.

Vieira, J., Carvalho, A., Campelo, F., 2020. Tree growth under climate change: evidence from xylogenesis timings and kinetics. Front. Plant Sci. 11, 1–11. https://doi.org/10.3389/fpls.2020.00090.

Wigley, T.M.L., Briffa, K.R., Jones, P.D., 1984. On the average value of correlated time series, with applications in Dendroclimatology and hydrometeorology. J. Clim. Appl. Meteorol. 23, 201–213. https://doi.org/10.1175/1520-0450.

Willmott, C.J., Feddema, J.J., 1992. A more rationale climatic moisture index. Prof. Geogr. 44, 84–87.

Zang, C., Biondi, F., 2015. treeclim: an R package for the numerical calibration of proxy-climate relationships. Ecography 38, 431–436.

Zhu, L., Cooper, D.J., Yuan, D., Li, Z., Zhang, Y., Liang, H., Wang, X., 2020. Regional scale temperature rather than precipitation determines vessel features in earlywood of Manchurian ash in temperate forests. J. Geophys. Res. Biogeosci. 125 e2020JG005955.